 FDMP, vol.1, no.2, pp.131-151, 2005

Locomotion of a Viscous Drop, Induced by the Internal Secretion of Surfactant: Boundary Effects

O.M. Lavrenteva [1], D. Tsemakh and A. Nir

Abstract: We have studied the motion of a drop, induced by the internal secretion of a surface-active substance, in the vicinity of solid walls or non-deformable liquid-liquid interface under micro-gravity conditions. The secreted substance renders a non-uniform distribution of surfactant along the outer surface that, in turn, results in interfacial stress variation that ultimately leads to a surface motion and to locomotion of the drop. Cases of plane and spherical boundaries have been considered as well as cases of linear and non-linear dependence of the interfacial tension on concentration of surfactant. The dependence of the drop migration velocity on the location of the source and on the separation distance between the drop and the outer boundary as well as on the physical parameters of the system is reported. The dynamics of the drop is studied in the case of a fixed location of the source inside the drop, and in the case when it passively moves with the internal circulation.

keyword: Viscous flow, drop, surfactant, locomotion, Marangoni effect

1 Introduction

Many modern industrial applications involve drops motion in a liquid matrix accompanied by heat or mass transfer between the phases. These include, e.g. direct heat exchange or liquid-liquid extraction. Exchange of active species with an ambient media is also one of the most characteristic features of living biological bodies. Most of the theoretical studies of such processes were based so far on the assumption of a uniform concentration or temperature inside the drops. This assumption does not hold in the case when a dissolved substance is secreted from some internal source within a drop, e.g. from an encapsulated smaller drop in the course of technological processes involving compound drops, or from certain organelles in a living cell. When a dissolved substance is secreted from an internal source within a drop that itself is embedded in a viscous fluid, concentration variations at the surface result in surface tension gradients that induce surface flow and locomotion of the drop in the viscous domain is realized. An internal secretion of active substance is typical especially for small biological bodies. The described system may thus serve as a simplified quantative model for chemotaxis of biological particles due to the activity of internal organelles such as mitochondria, lysosomes, and Golgi aparata.

A theoretical model for the motion of a drop due to the internal secretion of a surface-active substance was suggested by Nir and Lavrenteva (2003). In the model we considered a viscous drop that is embedded in an immiscible viscous fluid and contains another smaller droplet or a point source of a surface-active substance. The inner droplet is assumed to have a uniform concentration of the secreted material, while a non-adsorbing kinetics is used for the mass flux across the outer surface. Tsemakh, Lavrenteva and Nir (2004) have studied the locomotion of such compound viscous drop embedded in an unbounded viscous fluid. It was revealed that the internal secretion from the inner droplet induces locomotion of the compound viscous drop and that the inner circulation generated by the motion of the interface of the large drop causes a migration of the internal droplet in the same direction. In general it was found that the velocity of the inner droplet exceeds that of the large drop. With the passage of time, the droplet approaches the interface of the drop and the eccentricity of the system is increased. When the distance between the centers increases, the relative velocity first grows, but as the droplet approaches the interface, its relative motion is retarded by the strong viscous resistance. At the limiting configuration of the touching droplets the aggregate will move with a constant speed.

The combined effect of buoyancy and spontaneous Marangoni motion was studied as well. It was shown that a rich variety of interaction patterns may occur, which exhibits separation of flow in various domains. In some

[1] Chemical Engineering Dept, Technion, Israel.

particular cases both drops remain suspended motionless in the laboratory reference frame with the fluid circulating in a steady manner. A pair of drops may have several equilibrium positions, with one or two of them being stable. Thus, it was demonstrated that in the absence of external forcing an internal secretion of surfactants results in a spontaneous self-propulsion of the drop within an unbounded fluid with considerable velocities and that the flow induced by the Marangoni effect may substantially alter the flow pattern and migration velocity of drops that are under the influence of buoyancy.

However, in real applications, especially biological, the motion in an unbounded medium is not the typical case but, rather, it occurs in domains confined by various kinds of boundaries. The aim of this work is to extend the results of Tsemakh, Lavrenteva and Nir (2004) to these more physically relevant situations and to study the effect of nearby solid walls, free surfaces and liquid-liquid interfaces on the locomotion of a drop induced by the internal secretion of surface-active substance. The effect of non-linear dependence of the surface tension on a surfactant concentration is studied as well. Our focus is on the case when the dimension of the inner droplet is significant less than that of the large one and it is natural to model it by a point mass source with a given strength.

In section 2 the basic assumptions of our model are discussed and a mathematical formulation of the problem is presented. A spherical drop containing a source of a soluble weak surfactant, which is submerged into an immiscible viscous fluid, is considered. A point source model is assumed, neglecting the internal structure of an organelle and its dimension compared to that of the body. The outer fluid is confined by a flat or spherical boundary, where conditions of insulation or constant concentration are imposed. Three different types of outer boundary are considered: solid wall, free surface and liquid-liquid interface. All physical properties of the fluids are assumed to be constant except for the interfacial tensions, which are assumed to depend on the surface concentration. At the outset, we introduce dimensionless variables based on the size of the drop and the physical properties of the ambient fluid. The system is governed by the following set of dimensionless parameters: Reynolds number, Peclet number, capillary number, and the ratios of physical characteristics of the phases (viscosity, diffusivity).

The effects of inertia, convective transport and deformation were discussed in Tsemakh, Lavrenteva and Nir (2004) for the locomotion of a drop in an unbounded medium and were shown to exert only minor influence on the motion induced solely by the Marangoni force. It is anticipated that for the motion retarded by the boundaries, the effect of inertia and convective transport are even smaller than in unbounded media. In contrast to this, the deformations of the drops in the presence of boundaries may be more pronounced than in an unbounded fluid. Nevertheless, here, for simplicity, we consider the cases when all the effects mentioned above can be neglected, i.e. the Reynolds, Peclet and capillary numbers are assumed to be zero. Under these conditions the quasi-steady approximation is valid, i.e. the concentration and velocity fields can be found from stationary equations (Laplace and Stokes, respectively). The problems remain coupled only through the dependence of interfacial stress conditions on the variation of surfactant concentration at the surface. The method of solution (based on some earlier results concerning drop motion in the vicinity of flat boundaries, see Haber, Hetsroni and Solan, 1973, Keh and Chen, 1990, Loewenberg and Davis, 1993) is described in section 3.

The velocity and pressure fields in each phase satisfy the quasi-stationary Stokes equations with the following boundary conditions: The fluid is at rest at infinity. No-slip conditions are imposed on solid walls. The velocity field is continuous across each fluid interface. While the drops do not deform the difference of tangential stresses at the interfaces is balanced by the gradient of the surface tension. The problem definition is complemented by the balance of the forces acting on each of the drops from which the dynamics is extracted, and by the equations for temporal evolution of the positions of the drop and the internal source. The latter may be either fixed within the drop or passively migrating with the internal circulation.

The above problem is solved for axisymmetric configurations using conformal mapping techniques. In this procedure we first calculate the concentration distribution and the Stokes stream function from which the force on the drop can be obtained as a sum of Marangoni force, Stokes drag and buoyancy. Balancing these forces provides an equation on the drop's migration velocity that is used to advance the geometry of the system.

The results of simulations are reported in section 4. The migration velocity of the drop in the vicinity of a no-slip flat surface and a spherical shell is computed as a func-

tion of separation distance for a variety of governing parameters in sections 4.1 and 4.2, respectively. The temporary evolution of drop's position and streamline patterns are illustrated by characteristic samples. The extension of these results to the cases of a flat liquid-gas and liquid-liquid interface are described in sections 4.3. In section 5 we summarize the results of the simulations and compare the influence of nearby surfaces on the locomotion of a drop induced by internal secretion of surfactants to that obtained for other types of motion of drops available in the literature, e.g. sedimentation and thermocapillary migration under externally applied temperature gradient.

2 Problem formulation

Consider a drop of radius a submerged into an immiscible viscous fluid and containing a point source of a soluble weak surfactant of a constant flux Q. The outer fluid is confined by a spherical or flat boundary. The geometry of the system is illustrated in Figure 1.

All physical properties of the fluids are assumed to be constant, except for the interfacial tension on the drops' interface, which is considered to depend solely on the surface concentration of the active substance, $\sigma = \sigma(\Gamma)$. This dependence can be established experimentally or deduced theoretically from thermodynamic considerations (see e.g. Chen and Stebe 1997, and Edwards, Brenner and Wasan 1991). In practice, this dependence is often linearized to yield $\sigma = \sigma_0 + \sigma_\Gamma(\Gamma - \Gamma_0)$, where Γ_0 is a reference value and with σ_Γ being a constant.

At the outset, we introduce dimensionless variables based on the size of the drop and the physical properties of the ambient fluid, which are marked by a subscript 0. The properties of the drop's medium and those of the outer fluid are marked by subscript 1 and 2, respectively. The bulk and surface concentrations are scaled by $C^* = Q/(4\pi aD)$ and $\Gamma^* = Q/(4\pi D)$, respectively, while the velocity is scaled by $V^* = \sigma'\Gamma^*/\eta_0$, where η_0 denotes the ambient fluid viscosity and σ' is a characteristic/averaged magnitude of the surface tension derivative with respect to concentration. The system is governed by the following set of dimensionless parameters: the ratios of viscosities of the phases, $\mu_i = \eta_i/\eta_0$ (i=1,2), the ratio of the diffusivities of the phases $\kappa = D_1/D_0$,the Reynolds number, $Re = \rho_0 aV^*/\eta_0$, where ρ_0 is the density of the ambient phase; the capillary number $Ca_1 = \eta_0 V^*/\sigma_0$, and the Peclet number, $Pe = aV^*/D_0$. If the outer boundary is a liquid-liquid interface, its surface tension, σ_2, may depend on concentration and Marangoni flow may be induced at this interface as well. In the latter case, addressed below as a case of an active outer surface, additional parameter, $M_1 = \sigma'/\sigma_2'$, characterizes the relative intensity of the induced Marangoni flow at this interface.

As mentioned before, for simplicity, we consider the cases when inertia and convective transport and deformation effects can be neglected, i.e. negligibly small *Re* *Pe* and *Ca*

For any given configuration, the dimensionless concentration fields $c_i(\mathbf{x},t)$ satisfy Laplace equation

$$\nabla^2 c_i = 0, \quad \mathbf{x} \in \Omega_i \backslash \{\mathbf{x}_s\}, \quad i = 0, 1. \tag{1}$$

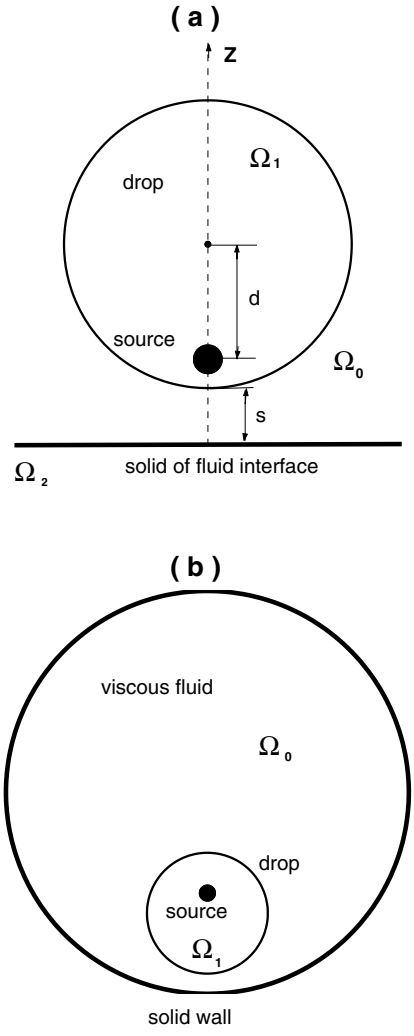

Figure 1 : A sketch of the geometry of the system

There is a point source of concentration at a given location inside the drop

$$c_1 \to \frac{1}{|\mathbf{x}-\mathbf{x_s}|}, \quad |\mathbf{x}-\mathbf{x_s}| \to 0. \tag{2}$$

We assume a local thermodynamic equilibrium between the surface and the bulk phases, yielding that the surface concentration of a surfactant is a function of the bulk one. These functional relations, which are addressed in the literature as adsorbtion isothermes, may be obtained experimentally or deduced theoretically from detailed microscopic analysis of adsorbtion-desorption (see e.g. Chen and Stebe 1997, and Edwards, Brenner and Wasan 1991). Further on, we assume the most simple linearized form of the adsorption isotherms, $c_i = k_i\Gamma$. It follows from these assumptions that the equilibrium bulk concentrations at the interface are proportional, $c_1 = (k_1/k_0)c_0$. For the simplicity of presentation we introduce a modified concentration $\overline{c}_0 = (k_0/k_1)c_0$ in the continuous phase and $\overline{c}_1 = c_1$ in the dispersed phase, which is continuous across the interface. Further on, the bars are omitted. Note that this transformation is equivalent to different scaling of concentration in the two phases. Since the surface concentration is proportional to the continuous bulk concentration, it is possible to consider the dependence of surface tension on this concentration c. Thus, the surface concentration is excluded from the formulation of the problem.

The modified concentration and the mass flux are continuous through the surface of the drop, i.e.,

$$c_1 = c_0, \quad \frac{\partial c_0}{\partial n} = \kappa\frac{\partial c_1}{\partial n}, \quad \mathbf{x} \in \partial\Omega_1, \tag{3}$$

while, at the outer boundary, either the concentration is constant

$$c_0 = 0, \quad \mathbf{x} \in \partial\Omega_0, \tag{4}$$

or the mass flux vanishes

$$\frac{\partial c_0}{\partial n} = 0, \quad \mathbf{x} \in \partial\Omega_0. \tag{5}$$

The velocity, $\mathbf{u}$, and pressure (modified by adding the gravity force potential), p, fields in each phase satisfy the quasi-stationary Stokes equations

$$\mu_i\nabla^2\mathbf{u}_i = \nabla p_i, \quad \nabla\cdot\mathbf{u}_i = 0, \quad \mathbf{x} \in \Omega_i, \quad i = 0,1,2, \tag{6}$$

and the following boundary conditions are applied at the drop's interface: the velocity field is continuous

$$\mathbf{u}_0 = \mathbf{u}_1, \quad \mathbf{x} \in \partial\Omega_1, \tag{7}$$

The normal components of the velocity of the fluid at the surface of a drop and of the velocity of the drop, $\boldsymbol{V}$,are equal

$$\mathbf{V}\cdot\mathbf{n} = \mathbf{u}_0\cdot\mathbf{n}, \quad \mathbf{x} \in \partial\Omega_1, \tag{8}$$

The balance of tangential stresses at the interface reads

$$\Pi^1_\tau - \Pi^0_\tau = \frac{\partial\sigma}{\partial\tau} = \frac{\partial\sigma}{\partial c}\frac{\partial c}{\partial\tau}, \quad \mathbf{x} \in \partial\Omega_1. \tag{9}$$

Here τ denotes an element tangential to the interface and $\Pi^i_\tau = \Pi^i{:}\,\mathbf{n}\tau$, where $\Pi^i = -p_i\mathbf{I} + \mu_i\left[\nabla\mathbf{u}_i + (\nabla\mathbf{u}_i)^T\right]$ is the stress tensor, while $\mathbf{n}$ and τ are unit vectors normal and tangential to the surface.

If the outer boundary is solid, a no-slip condition is imposed

$$\mathbf{u}_0 = 0, \quad \mathbf{x} \in \partial\Omega_0, \tag{10}$$

while at an outer free surface we set

$$\Pi^0_\tau = \frac{\partial\sigma_2}{\partial\tau}, \quad \mathbf{u}_0\cdot\mathbf{n} = 0, \quad \mathbf{x} \in \partial\Omega_0. \tag{11}$$

where σ_2 denotes the surface tension at $\partial\Omega_0$. In the case of a liquid-liquid interface $\partial\Omega_0$, the problem formulation is modified in a natural way. Equation (4) and (6) are solved in the domain of the third phase $\Omega_2 = \mathbf{R}^3\backslash(\Omega_0 \cap \Omega_1)$ and boundary conditions at $\partial\Omega_0$ are replaced by those similar to the conditions at $\partial\Omega_1$.

The balance of the forces acting on the drop reads

$$F = \oiint_{\partial\Omega_1}\Pi^0\bullet\mathbf{n}ds = 0, \tag{12}$$

while the temporal evolution of the position of the center of the drop is governed by

$$\dot{\mathbf{Z}} = \mathbf{V}, \quad \mathbf{Z}(0) = \mathbf{Z}^0. \tag{13}$$

The source position inside the drop, $\mathbf{x}_s$(t), can be either fixed with respect to drops surface, or it may move passively with the flow. In the first case, the equation of source motion is similar to (13)

$$\dot{\mathbf{x}}_s = \mathbf{V}, \quad \mathbf{x}_s(0) = \mathbf{x}^0_s, \tag{14}$$

while in the second case, the drop's velocity should be replaced by the velocity of the liquid at a corresponding point

$$\dot{\mathbf{x}}_s = \mathbf{u}(\mathbf{x}_s(t),t), \quad \mathbf{x}_s(0) = \mathbf{x}_s^0. \tag{15}$$

We are interested also in the position of the source inside the drop relative to its center, $\mathbf{d}(t) = \mathbf{x}_s(t) - \mathbf{Z}(t)$. Obviously, in the case of a fixed source $\mathbf{d}$ does not depend on time.

The formulation of the problem is completed by specifying dependence of the surface tension on concentration. Most of our results are computed under assumption that this dependence is linear

$$\sigma = \sigma_0 - \sigma'(c - c^0), \tag{16}$$

which provides a good approximation for moderate values of concentration and small variations along the interface. However, for high concentrations, the change of surface tension with concentration considerably slows down (see e.g Adamson, 1990). To describe this phenomenon we admit a quasi-linear model: The dependence of surface tension on concentration is divided to two different regions: In the first region the dependence is strong and can be described by (16), while in the second region, where the surface tension is low, its change with concentration is very slow and it can be approximated by a constant,

$$\sigma = \begin{cases} \sigma_0 - \sigma'(c - c^0), & c < c^1 = c^0 + (\sigma_0 - \sigma_1)/\sigma', \\ \sigma_1 & c \geq c^1. \end{cases} \tag{17}$$

Most of the calculations presented in this paper are performed under the assumption of a linear surface tension (16). A detailed study of the effect of non-linear surface tension (17) was carried out for the case of an insulated plane wall and it is anticipated to be qualitatively the same in the other cases.

3 Method of solution

Under the quasi-stationary approximation, the concentration field resulting from problems (1) – (4) or (1) - (3), (5) may be solved for any given configuration of the system, independent of the hydrodynamic part, and provide the distribution of concentration on the interface $\partial\Omega_1$. As soon as the latter is known, the velocity field can be obtained for any given velocity of the drop, $\mathbf{V}$, by solving (6) – (11). Finally, a use is made of the linearity of creeping flow to find the migration velocity from the net force balance (12).

If the motion of the droplet is axi-symmetric, as it is in the case of the motion driven solely by the Marangoni effect, it is convenient to apply orthogonal coordinates, (ξ,ζ,ϕ), conjugate to the cylindrical system (z,r,ϕ), having the interface of the drop and the outer boundary as coordinate surfaces and to introduce an axi-symmetric Stokes stream function Ψ such that the velocity components are

$$u_\xi = \frac{h}{r}\frac{\partial \Psi}{\partial \zeta}, \quad u_\zeta = -\frac{h}{r}\frac{\partial \Psi}{\partial \xi}$$

where h is a metric coefficient.

The stream function satisfies the following equation (Happel and Brenner, 1965)

$$E^2\left(E^2\Psi_i\right) = 0, \quad \mathbf{x} \in \Omega_i, \quad i = 0,1. \tag{18}$$

with

$$E^2 = rh^2\left[\frac{\partial}{\partial \xi}\left(\frac{1}{r}\frac{\partial}{\partial \xi}\right) + \frac{\partial}{\partial \zeta}\left(\frac{1}{r}\frac{\partial}{\partial \zeta}\right)\right]$$

In this representation the subscripts 0 and 1 correspond to domains of the continuous outer phase with $\beta < \xi \leq \alpha$, and the droplet, $\xi > \alpha$, respectively. The boundary conditions at the interface of the drop can be rewritten in terms of the stream function as

$$\begin{aligned} &\Psi_0 = \Psi_1 = -r^2 V, \quad \frac{\partial \Psi_0}{\partial \xi} = \frac{\partial \Psi_1}{\partial \xi}, \\ &\Pi^0_{\xi\zeta} - \Pi^1_{\xi\zeta} = h\frac{\partial \sigma}{\partial \zeta}, \quad \xi = \alpha, \end{aligned} \tag{19}$$

while the conditions at the solid wall and free surface read

$$\Psi_0 = 0 \quad \text{and} \quad \frac{\partial \Psi_0}{\partial \xi} = 0, \quad \xi = \beta, \tag{20}$$

or

$$\Psi_0 = 0 \quad \text{and} \quad \Pi^0_{\xi\zeta} = M_1 h\frac{\partial \sigma_2}{\partial \zeta}, \quad \xi = \beta, \tag{21}$$

respectively.

As soon as the stream function is known, the force exerted on a body by the fluid in the positive z-direction can be calculated following Happel and Brenner, 1965, as

$$\mathbf{F} = \mu\pi\mathbf{e}_z \int r^3 \frac{\partial}{\partial\xi}\left(\frac{E^2\Psi}{r^2}\right) d\zeta. \tag{22}$$

Due to the linearity of the problem, the flow field may be constructed as a superposition of a Marangoni flow generated around the interface of the drop at rest by a given distribution of surfactants and a flow that would be generated by the motion of the drop in the absence of the Marangoni effect. Similarly, the force acting on the drop can be represented as a sum of the following forces:

1. Marangoni force F_m that is exerted on the drop at rest by a flow generated by a non-uniform distribution of concentration. Supposing V = 0 in boundary condition (19) we solve the system of equations (18) – (20) or (18), (19), (21) and then find the force $F_m$according to (22);
2. Hydrodynamic drag force,$\mathbf{V}F$, that acts on a moving drop in the absence of the Marangoni effect. Fcan be found by applying (22) to the solution of (18) – (20) or 18), (19), (21) with $V = 1$ and with $\frac{\partial\sigma}{\partial\zeta} = 0$ in boundary condition (19).

If the drop does not touch the outer surface, the migration velocity V is found from the balance of the forces acting on the drop as

$$V = -\frac{F_g + F_m}{F}. \tag{23}$$

When the separation between the interfaces is larger than or comparable with the dimension of the drop, the natural choice is to use the bi-spherical coordinate system (ξ,ζ,ϕ) connected with the two droplets that is linked with the cylindrical system by the following relations:

$$z = \frac{\sinh\xi}{h}, \quad r = \frac{\sin\zeta}{h}, \quad h = \frac{1}{\sinh\alpha}(\cosh\xi - \cos\zeta).$$

The interfaces of the drop and the outer boundary are described by the coordinate surfaces $\xi = \alpha \geq 0$ and $\xi = \beta < \alpha$, respectively. If the outer boundary is a plane z = 0, then $\beta = 0$ and α can be defined from

$$\cosh\alpha = s + 1,$$

where s is a given separation distance between the drop and planar surface. In the case of a spherical outer boundary, α and β can be determined by

$$\cosh\beta = \frac{(1-R+s)^2 + 1 - R^2}{2(1-R+s)},$$

$$\cosh\alpha = \frac{1 - R^2 - (1-R-s)^2}{2R(1-R-s)}, \quad 0 < \beta < \alpha,$$

with R being the radii ratio.

It is convenient to present the concentration as a sum

$$c_i = G(\mathbf{x}, \mathbf{x_s}) + b_i(\mathbf{x}), \quad i = 0, 1,$$

where $G(\mathbf{x}, \mathbf{x_s})$ is a Green function for Poisson equation in half space with boundary conditions (4) or (5), while b_i is a bounded harmonic function in Ω_i satisfying the boundary conditions (4) or (5) at $\partial\Omega_0$ and

$$b_0 = b_1 \quad \text{and} \quad \frac{\partial b_0}{\partial n} - \kappa\frac{\partial b_1}{\partial n} = (1-\kappa)\frac{\partial G(\mathbf{x}, \mathbf{x_s})}{\partial n}, \quad x \in \partial\Omega_1. \tag{24}$$

The general solution of the Laplace equation is expressed in the form of Fourier series (see e.g., Subramanian and Balasubramaniam, 2001)

$$b_i = (\cosh\xi - \cos\zeta)^{1/2} \times \sum_{n=1}^{\infty} \left[\begin{array}{l} E_n^i \cosh(n+1/2)\xi \\ +G_n^i \sinh(n+1/2)\xi \end{array} \right] P_n(\cos\zeta), \quad i = 0, 1, \tag{25}$$

where $P_n(\mu)$ are Legendre polynomials. Substituting these series into boundary conditions (24) and (4) or (5) results in an infinite system of linear algebraic equations for the coefficient E_n^i and G_n^i, which we then solve for a specified level of accuracy (see Appendix for more details). Note that, in a special case κ = 1, the solution for concentration can be obtained in an explicit form as

$$c_i = G(\mathbf{x}, \mathbf{x_s}) = \frac{1}{|\mathbf{x} - \mathbf{x_s}|} \pm \frac{1}{|\mathbf{x} - \mathbf{x}_m|}, \quad \mathbf{x} \in \Omega_i, \quad i = 0, 1, \tag{26}$$

where $\mathbf{x}_m$ is a mirror image of $\mathbf{x}_s$ with respect to $\partial\Omega_0$, while '+' and '-' signs reflect insulation and constant concentration on $\partial\Omega_0$.

As soon as the concentration field is available, the stream function can be determined using the algorithm developed for computing the interaction of a drop and a plane surface under Marangoni convection (Barton and Subramanian, 1990).

The general solution of (18) in bi-spherical coordinates was given by Stimson and Jeffery (1926) as

$$\Psi_i = (\cosh\xi - \mu)^{-3/2} \sum_{n=1}^{\infty} W_n^i(\xi) C_{n+1}^{-1/2}(\mu), \quad i = 0, 1, \tag{27}$$

where $C_{n+1}^{-1/2}(\mu)$ are the Gegenbauer polynomials and with the general form of the coefficients W_n^i being

$$W_n^i = A_n^i \cosh(n-1/2)\xi + B_n^i \sinh(n-1/2)\xi + C_n^i \cosh(n+3/2)\xi + D_n^i \sinh(n+3/2)\xi \tag{28}$$

Substituting (27) and (28) into boundary conditions (19) – (21) results in a finite system of linear equations for the coefficients of the stream function for any choice of n. The right-hand side of this system depends on the coefficients E_n^i and G_n^i, (see Golovin, Nir and Pismen, 1995, and Appendix for the details). The force exerted on the drop by the flow can be computed according to Happel and Brenner (1965).

$$F = \frac{2\pi\mu_0\sqrt{2}}{\sinh\alpha} \sum_{n=1}^{\infty} \left(A_n^0 + B_n^0 + C_n^0 + D_n^0\right).$$

As soon as the Marangoni force, F_m, and viscous resistance, F, are known, the migration velocity is found from (23) and the drop's position is updated according to (13). For the problem with a free suspended source, representation (27), (28) with computed coefficients is used to determine the velocity of the source, the position of which is then updated according to (15).

4 Results of simulations

The crucial part of the solution of the problem is the determination of the migration velocity for a given geometry of the system that is characterized by separation distance, s, and position of the source inside the drop, d. In this section we present a parametric analysis of this auxiliary problem for various types of outer boundaries and several characteristic samples of dynamic calculations.

4.1 Plane solid wall

4.1.1 Migration velocity and velocity of the source

The velocity of the drop and the relative velocity of the source within the drop in the vicinity of a plane solid wall $z = 0$ (see Figure 1a) are plotted versus the separation distance in Figs 2 and 3, respectively. Figs (a) and (c) correspond to an insulated wall, while (b) and (d) correspond to a constant concentration at $\partial\Omega_0$.

The dependence of the velocity on the separation distance between the drop and the wall, $s = Z - 1$, and on the position of the internal source, d, is illustrated in Figs (a) and (b) for a fixed viscosity ratio $\mu_1 = 0.1$. Various curves correspond to various positions of the source. The value of d is positive when the source is located above the center of the drop and it is negative in the opposite case (see Figure 1). d= 0 corresponds to the source located at the center of the drop. Similarly, V is positive when the drop migrated from the wall and negative in the opposite case, while at the equilibrium position V= 0. Curves 1, 2, 3, 4, and 5 in Figs (a) and (b) correspond to d= 0.8, 0.3, 0, – 0.3 and – 0.8, respectively.

One can see that if the source is located near the upper interface (see curves 1) the drop migrates from the wall, while the free source will move toward the upper surface. These velocities grow monotonically with the separation distance up to the value of the velocity in an unbounded fluid far from the wall. When the source is located further from the surface above the drops center (see curves 2), the dependence of the velocity on the separation distance is no more monotonic. For an insulated wall, Figs (a), for very small separations the velocities are negative, i.e. the drop is attracted to the wall and the free source approaches the lower interface. At a certain distance, the migration velocity vanishes and for larger separations the velocity increases monotonically, while the free source approaches the upper interface. For the fixed source this critical distance corresponds to an unstable equilibrium configuration. In contrast to this, near a wall with a constant concentration (Figs. b), the velocities are always positive (i.e. the drop moves from the wall and the free source migrates to the upper surface) and achieve their maximum values at a certain (different) separation distances and then reduce to an asymptotic value, which conforms to the value of the velocity in an unbounded fluid.

A source located at the center (lines 3) induces a uniform

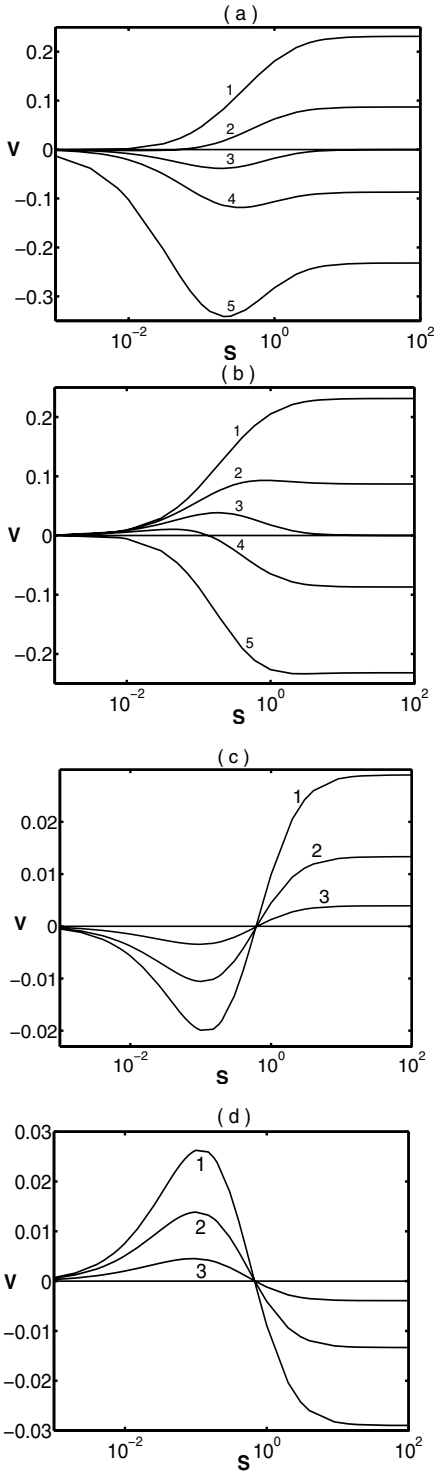

Figure 2 : Migration velocity of a drop near a solid wall with a zero mass flux (a and c) or uniform concentration (b and d) versus separation distance. $\kappa = 1$. (a) and (b): $\mu_1 = 0.1$, curves 1, 2, 3, 4, and 5 correspond to $d = 0.8$, 0.3, 0, – 0.3 and – 0.8, respectively. For (c) $d = 0.1$ and for (d): $d = -0.1$, while curves 1, 2, and 3 correspond to $\mu_1 = 0.1$, 1, and 5, respectively.

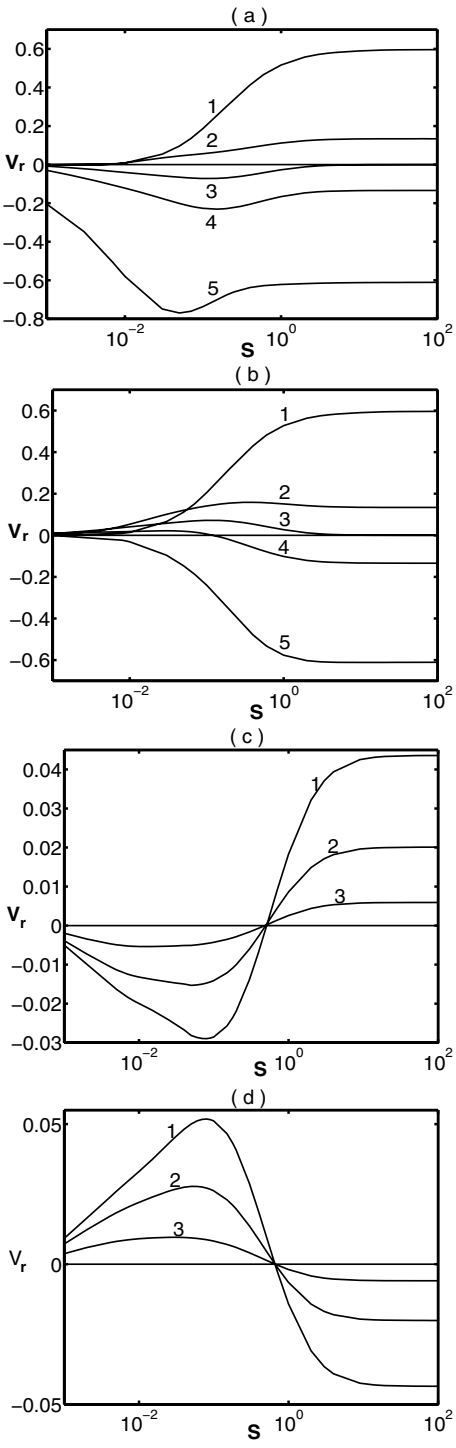

Figure 3 : Relative migration velocity of a free source inside a drop near a solid wall with a zero mass flux (a and c) or uniform concentration (b and d) versus separation distance. $\kappa = 1$. (a) and (b): $\mu_1 = 0.1$, curves 1, 2, 3, 4, and 5 correspond to d= 0.8, 0.3, 0, – 0.3 and – 0.8, respectively. For (c) $d = 0.1$ and for (d): $d = -0.1$, while curves 1,2, and 3 correspond to $\mu_1 = 0.1$, 1, and 5, respectively.

distribution of concentration at the interface of the drop in an unbounded fluid and no Marangoni flow occurs in this case. The presence of a nearby wall breaks the symmetry and thus results in the migration of such a drop. Our calculations reveal that a drop with a source at the center is attracted to an insulated wall, while the relative velocity at its center is negative, Figs. (a). In contrast to this, the drop is repulsed from the wall with constant concentration having a positive velocity at the center, Figs. (b). In both cases the migration velocity vanishes at near contact and at large separations, while the velocity at the center tends to a constant value at a near contact configuration.

If the source is located lower than the center (lines 4 and 5), then the drop always moves towards an insulated wall and the free source approaches the lower interface, Figs. (a), while for the wall with uniform concentration, Figs. (b), there may exist critical separations when the drop migration velocity and the velocity at the location of the source vanish. Note that, generally, these two critical separations are different. The first critical separation describes a stable equilibrium position of the drop with a fixed source, such that the drop is attracted at higher separations and repulsed for lower ones. A stable equilibrium of a drop with a free source is possible only for very special conditions when the two velocities, of the drop and of the source vanish simultaneously. At near contact configuration, the migration velocity vanishes, while the velocity at the source location tends to some non-zero value.

The dependence of the migration velocity and the velocity at the location of the source on the viscosity ratio is illustrated in Figs. (c) and (d), where curves 1, 2 and 3 correspond to viscosity ratio 0.1, 1 and 5, respectively. The distance between the source and the center of the drop d= 0.1 and – 0.1 for Figs. (c) and (d), respectively. It is evident that, for an insulated wall, Figs. (c), closer drops are attracted to the wall while the free sources within them migrate to the lower surface. In contrast to this, more distant drops are repulsed and the velocities at the source locations are positive. At a certain separation, a little smaller than the drop's radius, the drop's velocity vanishes. This separation corresponds to an unstable equilibrium of a drop with a fixed internal source. For a wall with uniform concentration (Figs. d), the drop is attracted for large separation and repulsed for smaller ones, while the relative velocity at the location of the source is positive for small separations and negative for larger. At a critical separation, the drop with a fixed source is at a stable equilibrium position. The magnitude of the both velocities decreases with the viscosity ratio, and vanishes at $\mu_1 \to \infty$, a limit that corresponds to the case of a solid particle. At an opposite limiting case$\mu_1 \to 0$, describing a gas bubble or an inviscid drop, the migration velocity tends to some finite value. An equilibrium separation turns out to be almost independent of the viscosity ratio.

4.1.2 Effect of a non-linear surface tension

The results of the previous section were calculated for a linear dependence of surface tension on concentration (16), which provides a good approximation for moderate values of concentration and small variations along the interface. However, for higher concentrations that are typical when the source is located near the interface, the change of surface tension with concentration slows down considerably (see e.g. Adamson, 1976). To describe this phenomenon we admit a piecewise-linear model (17), where the surface tension remains a low constant, when concentration exceeds some critical value c^1. Obviously, if the concentration at the entire interface in less than c^1, the results do not differ from those obtained for the linear surface tension. In the opposite case, when the concentration at the entire interface exceeds c^1, the surface tension is uniformly constant and no Marangoni flow takes place.

The effect of a non-linear surface tension is illustrated in Fig.4, where the migration velocity is plotted versus the distance between the drop's center and the source for various positions of the drop relative the wall and various values of a critical concentration c^1. The case of linear surface tension is presented by curves 4, while curves 1, 2 and 3 correspond to c^1 = 0.5, 0.7 and 1, respectively. Curves in plot (a) and (c) are calculated for the case of large separation distance $s > 5$, where the influence of the wall is negligibly small. These curves are almost the same for insulated and constant concentration boundary conditions and coincide with those computed for an unbounded outer medium.

Results for smaller separation distance $s = 0.3$ when the influence of the wall is significant are presented in Figs 4 (b) and (d) for a constant concentration and insulation conditions, respectively. As anticipated, for high critical concentration and near-center position of the source, the concentration all over the surface does not exceed

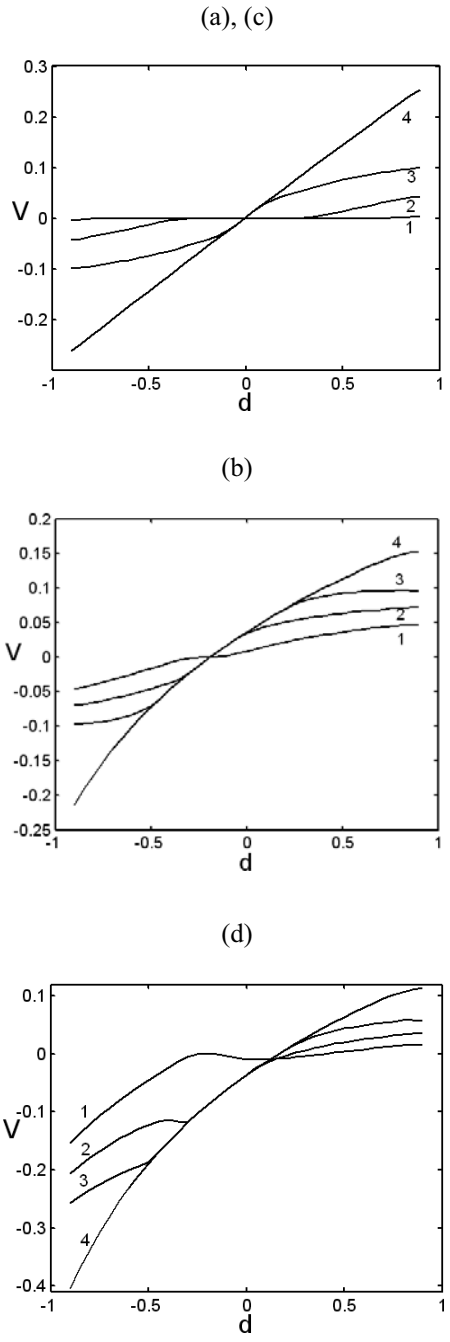

Figure 4 : Migration velocity of a drop located far from and near a solid wall versus the position of the source relative to the drop's center, μ_1=1 and κ = 1. (a) $s > 5$ and (b) s = 0.3, uniform concentration. (c) $s > 5$ and (d) s = 0.3, zero mass flux. Lines 1, 2, 3 and 4 denote c^1 = 0.5, 0.7, 1 and a linear surface tension, respectively.

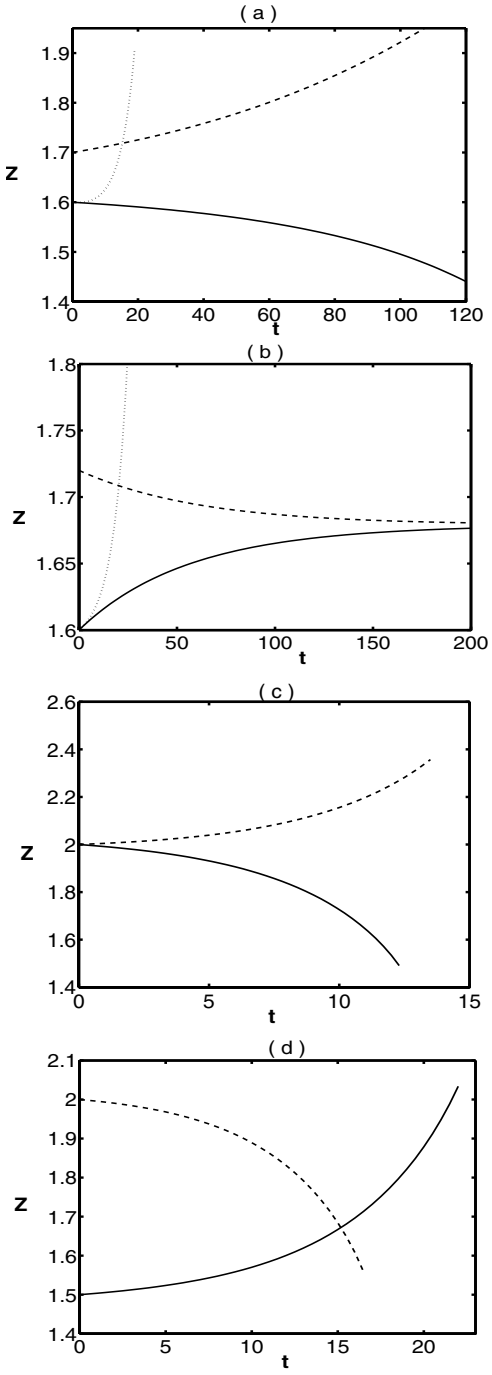

Figure 5 : Evolution of the drop's center position with time near a solid wall with zero mass flux (a and c) and constant concentration (b and d) for μ_1 = 1 and κ = 1. Solid and dashed curves (in (a) and (b)) denote cases with a fixed source position, while dotted curves reflect a freely suspended source. Curves in (c) and (d) are computed for a freely suspended source. (a) d = 0.1; (b) and (d) d_0= - 0.1; (c) d_0 = - 0.1 for the solid line and d_0 = 0 for the dashed curve.

the critical value and, hence the migration velocity is the same as in the linear case. When the source is located near the interface, a region with super critical concentration where surface tension gradient appears. In such cases, the migration velocity for the non-linear surface tension is lower than for the linear one. The slow down effect is much more pronounced when the source is located closer to the interface, in which case a larger part of interface has a high concentration.

Summarizing the results of the velocity calculations, one can conclude that a wall with zero mass flux attracts a drop undergoing spontaneous Marangoni migration, while a wall with a uniform concentration has a repulsive effect. On the other hand, the presence of a nearby solid wall results in an increase of the hydrodynamic resistance and, hence, leads to smaller migration velocities than those observed in an unbounded fluid.

4.1.3 Dynamics of the drops and flow patters

Typical examples of the evolution of the drop's center position with time near solid walls with zero mass flux and constant concentration are presented in Figs. 5a, 5c and 5b, 5d, respectively. All the curves in Fig 5 are calculated for μ_1=1 and κ = 1. In Fig. 5a the initial source position is d_0= 0.1; solid and dashed curves are computed for a fixed source position, $d(t) = d_0$ =0.1, with Z_0= 1.6 and 1.7, respectively. One can see that in the first case the drop approaches the wall while in the second case it moves away from it. This indicates that an equilibrium position between these two values is unstable. The dotted curve was calculated under the condition that the source is freely suspended within the drop and moves with the flow, i.e. $d(t)$was computed according to (15), while the initial conditions are the same as for the solid curve. In this case the source approaches the upper interface of the drop and the Marangoni effect becomes stronger with time that leads to the acceleration of the drop.

In Fig. 5b, the source is initially closer to the wall, d_0 =– 0.1. Again, solid and dashed curves are computed for the fixed source position, $d(t) = d_0$ =– 0.1, with Z_0= 1.6 and 1.72, respectively. In contrast to the motion near an insulated plane, which is illustrated in Fig. 5a, here drops which are initially located near the wall (solid curve) migrate away from the boundary, while those initially located further from the wall (dashed curve) are attracted to it. Such a behavior indicates the approach of the drop to a stable equilibrium position. The dotted curve was calculated under the condition that the source is freely suspended within the drop and illustrates and accelerated upwards motion of the drop due to the approach of the source to the upper interface of the drop.

In Figs. (c) and (d) both curves are calculated for a freely suspended source. In Fig 5c, the drop is initially separated by a distance of one radius from the wall, the dashed line corresponds to initially centered source, d_0 =0, while for the solid curves d_0 =– 0.1. Both the drop and the source migrate upwards in the first case and in the opposite direction in the second case. In Fig 5d, solid and dashed curves were calculated for d_0 =– 0.1 and Z_0= 1.5 and 2, respectively. Again, in both cases the drop and the source migrate in the same direction and the motion of the drop is accelerated. In contrast to the case of fixed source position (see Fig 5b), there is no equilibrium position of the drop. Various types of the flow induced by the motion of a drop in the vicinity of a solid wall are illustrated in Fig 6. All the streamlines were calculated for μ_1 = 1 and κ = 1. For figures of the left column (a, c and e) the solid wall is insulated, while for the rest of the figures (b, d and f) the uniform concentration condition is imposed. In Fig 6a the separation distance is s= 1, while the distance between the drop's center and the source is d =– 0.3. The drop migrates upwards from the wall and one can see two vortices in the flow. In Fig. 6b, where d= – 0.1 and s = 0.1, the drop migrates upwards from the wall and a single vortex is evident. A similar one vortex pattern that corresponds to the case when the drop moves towards the wall with a uniform concentration is illustrated in Fig. 6c, where $s = 0.5$, $d = -0.3$. In Fig. 6d, where $s = 1.7$, $d = -0.1$, the flow domain is separated into a vortex and a domain without closed streamlines. The streamline patterns around stationary drops are illustrated in Figs. (e) and (f), where $d = 0.21$, $s = 0.2$, and $d = -0.1$, s= 0.68, respectively. In both cases, a four vortices structure of the flow is evident, two of them inside the drop and another two in the outer fluid.

4.2 Spherical cavity

The velocity of the drop and the relative velocity of the source within a spherical cavity of $R = 5$ with constant concentration at the wall (see Figure 1b) are plotted versus the separation distance in Fig. 7. The position of the drop changes from near contact with the lower wall, s= 10^{-3}, up to a concentric position, s= 4. Velocities for

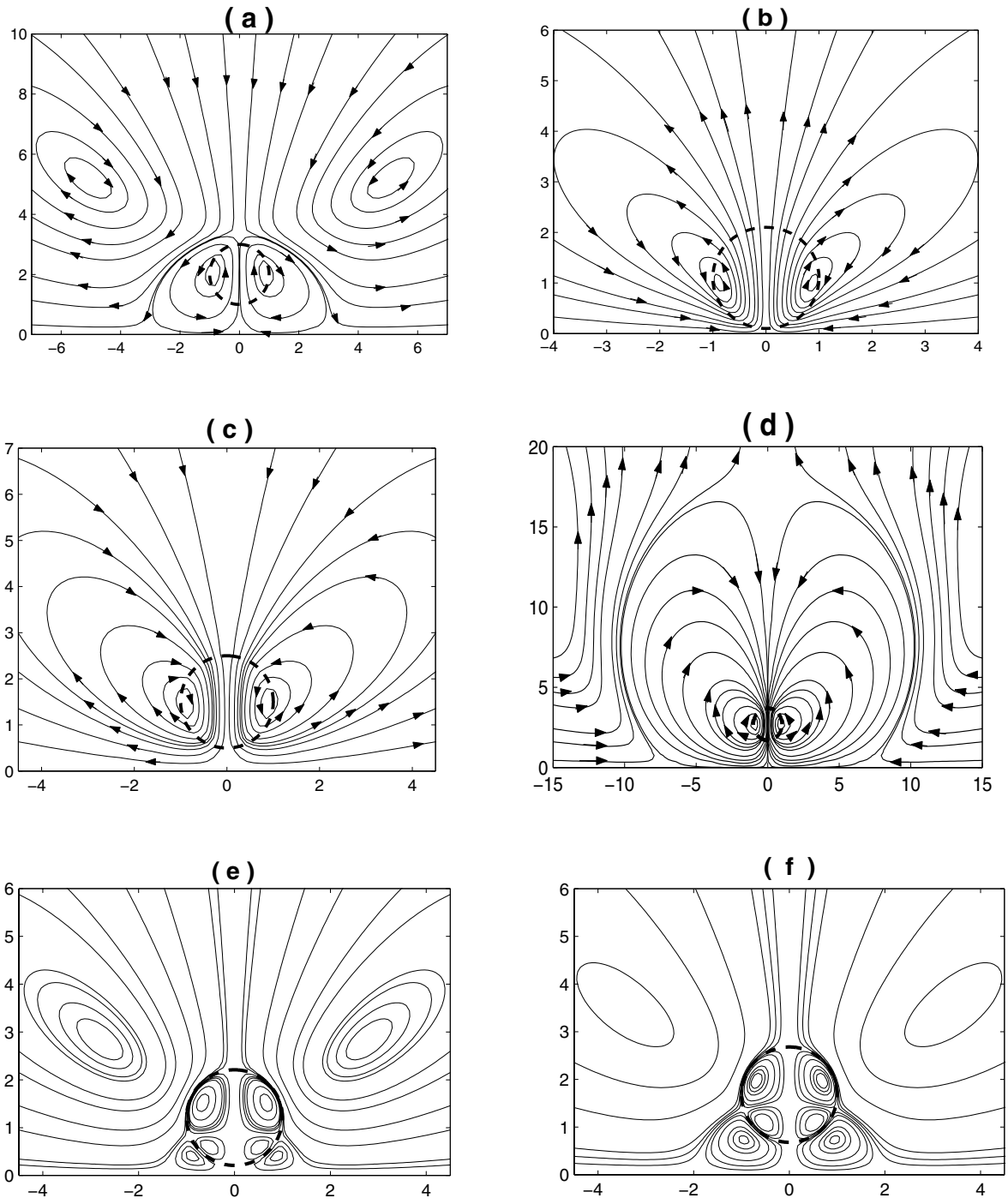

Figure 6 : Streamline patterns for a drop near a wall, $\mu_1 = 1$ and $\kappa = 1$. In (a), (c) and (e) the solid wall is insulated. In (b), (d) and (f) uniform concentration condition is imposed. (a) s= 1, d =– 0.3, (b) s= 0.1, d = – 0.1. In (a) and (b) the drop migrates upwards. (c) s = 0.5, d= – 0.3, (d) s= 1.7, d= – 0.1. In (c) and (d) the drop migrates downwards. (e) s = 0.21, d= 0.2, (f) d = – 0.1, s= 0.68, (e) and (f) show equilibrium positions.

the case when the drop is located above the center of the container can be obtained from simple symmetry considerations. Figs. (a) and (b) correspond to the velocity of the drop, while (c) and (d) correspond to the velocity of fluid at the location of the source. Curves 1, 2, 3, 4, and 5 in Figs. (a) and (c) were calculated for μ_1 = 0.1 and d= 0.7, 0.3, 0. – 0.3, and – 0.7, respectively. One can see that, similar to the case of a plane wall, if the source is located near the upper interface (see curves 1 and 2) the drop migrates from the wall, while the free source will move toward the upper surface. For a source position closer to the interface, curve 1, the velocity of the drop grows monotonically with the separation distance, while the velocity at the location of the source achieves a maximum value at some off-center position and then decreases. The latter type of behavior is typical for both velocities when the source is located closer to the center of the drop (see curves 2). A source located at the center (lines 3) induces the motion of the drop away from the nearest wall with constant concentration having a positive velocity at the center. Both velocities vanish at the symmetric configuration, when the drop is located at the center of the container, where a source induces a uniform distribution of concentration at the interface of the drop and no Marangoni flow occurs. If the source is located lower than the center (lines 4 and 5), then, again similar to the case of a plane wall, there may exist critical separations when the drop migration velocity and the velocity at the location of the source vanishes. Generally, these two critical separations are different. The first critical separation describes a stable equilibrium position of the drop with a fixed source, such that the drop is attracted at higher separations and repulsed for lower ones.

The dependence of the migration velocity and the velocity at the location of the source on the viscosity ratio is illustrated in Figs. 7b and 7d, where curves 1, 2 and 3 correspond to viscosity ratio 0.1, 1 and 5, respectively. The distance between the source and the center of the drop is d= 0.1 for Fig (c) and d= – 0.1 for Fig (d). It is evident that drops with small separation distance, s, are repulsed from the nearest wall while the free sources within them migrate upwards. In contrast to this, more distant drops are attracted and the velocities at the source locations depends on its position. At a certain separation, $s \sim 0.2$, the drop's velocity vanishes. This separation corresponds to a stable equilibrium of a drop with a fixed internal source. The magnitude of both velocities decreases with the viscosity ratio, and vanishes at $\mu_1 \to \infty$, which corresponds to the case of a solid particle. At an opposite limiting case $\mu_1 \to 0$, describing a gas bubble or an inviscid drop, the migration velocity tends to some finite value. The equilibrium separation turns out to be almost independent of the viscosity ratio.

Typical examples of the evolution of the drop's center position within a spherical shell are presented in Fig. 8. All the curves in Fig. 8 are calculated for $\mu_1 = 1$, $\kappa = 1$ and $d_0 = -0.1$; solid and dashed curves are computed for s_0= 0.3 and 0.8, respectively. In Fig 8a the source position is fixed, $d(t) = d_0 = -0.1$. One can see that in the first case the drop moves away from the wall while in the second case it migrates in the opposite direction. This indicated that an equilibrium position between these two values is stable. The curves in Fig 8b that were calculated under the condition that the source is freely suspended within the drop and moves with the flow, i.e. $d(t)$was computed according to (15) with the same initial conditions as for Fig. 8a, illustrate upwards and downwards accelerated motion of the u drop and no equilibrium is evident.

Various types of flow patterns induced by the motion of a drop within a spherical shell with constant concentration are illustrated in Figure 9. In Figure 9a the separation distance is s= 0.4 and an upward motion of the drop is evident, while Figure 9b illustrates a streamline pattern at an equilibrium separation s =0.536.

4.3 Free surface and a liquid/liquid interface

Free surface and a liquid/liquid interface differ from a solid wall in two main aspects: First, it is mobile, i.e. tangential velocity on the interface does not vanish and, hence, its retardation effect on the flow is less pronounced than that of a solid boundary. Second, its surface tension may depend on concentration as well. In this case, the Marangoni flow is induced not only at the vicinity of the drop, but also at the vicinity of the boundary. In what follows we address this type of interface as an active one in order to distinguish it from a passive interface with a constant surface tension. For mobile interfaces we restrict our considerations to the most physically relevant insulation condition at the interface.

The velocity of the drop in the presence of a plane interface $z = 0$ is plotted versus the separation distance in Figure 10. (a) and (b) correspond to an active surface of the drop with a passive outer boundary and to the opposite case, respectively.

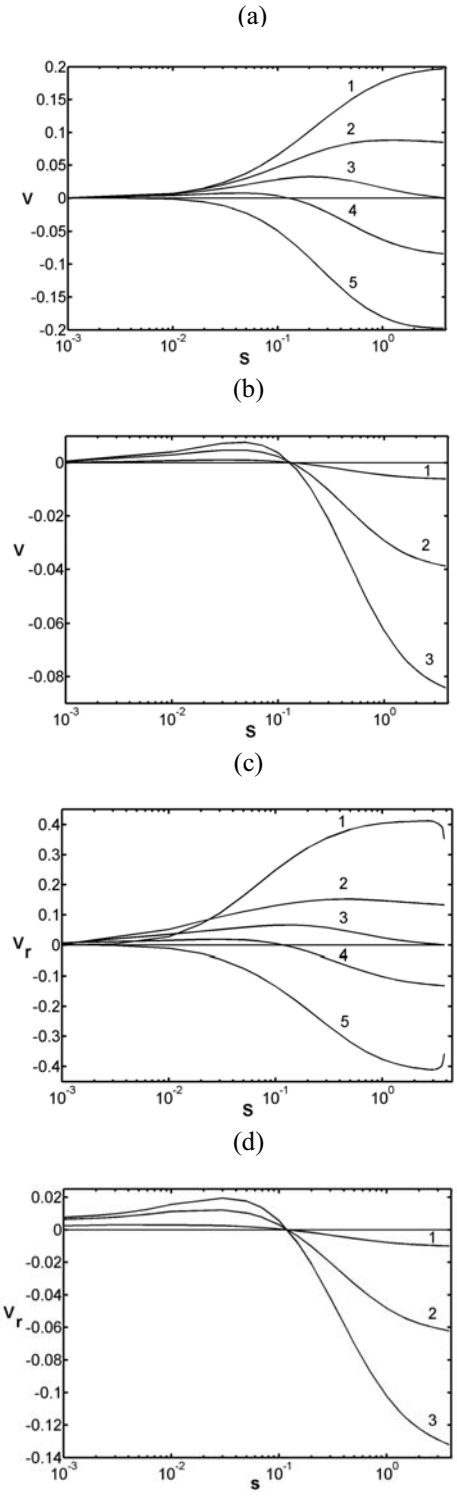

Figure 7 : Velocity of a drop (a and b) and of the source (c and d) versus separation distance. (a) and (c): μ_1=0.1, curves 1, 2, 3, 4, and 5 correspond to d = 0.7, 0.3, 0, –0.3 and – 0.7, respectively. (b): d = 0.1; (d): d = – 0.1. Curves 1, 2, and 3 correspond to μ_1=0.1, 1, and 5, respectively.

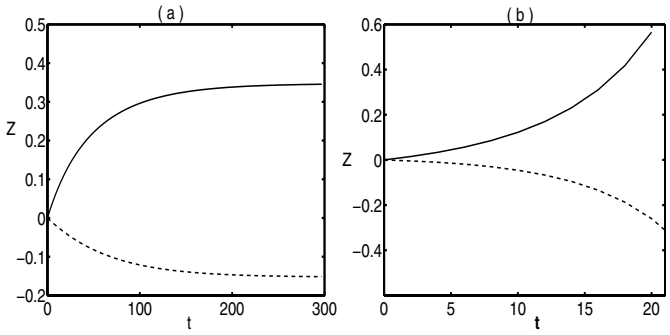

Figure 8 : Evolution of the drop's center position, $Z(t) - Z_{0,}$ with time inside of an insulated spherical cavity for μ_1=1, κ=1, d_0 =– 0.1. Solid and dashed curves are computed for s_0= 0.3 and 0.8, respectively. (a) The source position is fixed; (b) the source is freely suspended.

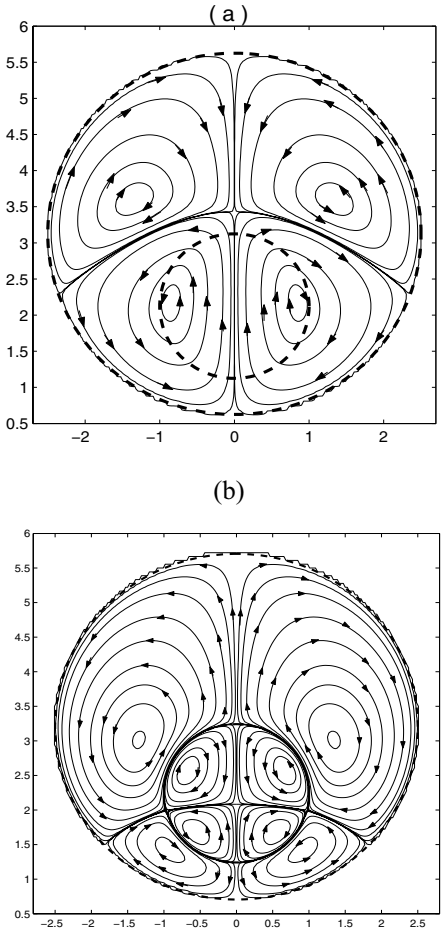

Figure 9 : Streamline patterns for μ_1= 1, κ = 1, R =2.5, d =– 0.1. The spherical solid wall is insulated. (a) upward motion of the drop at s = 0.4 approaching the equilibrium configuration. (b) stable equilibrium position at s =0.536.

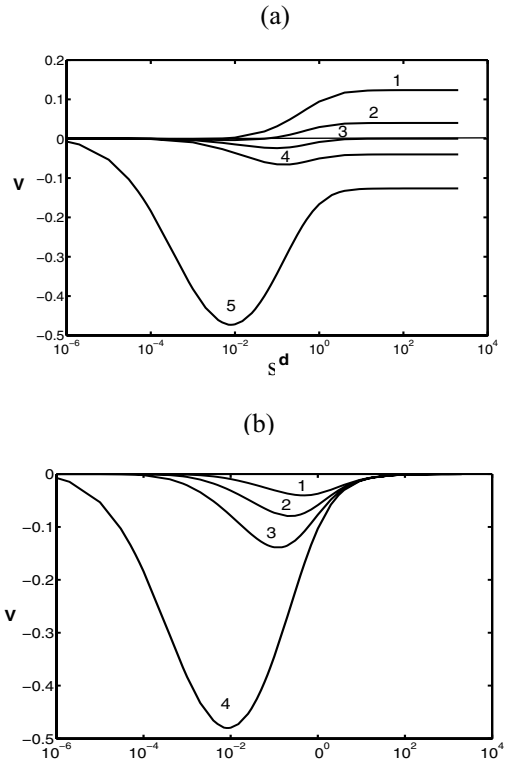

Figure 10 : Velocity of the drop versus separation distance $\mu_1 = \mu_2 = 1$ and $\kappa = 1$. (a) active surface of the drop. The curves 1, 2, 3, 4 and 5 correspond to d =1, 0.3, 0, – 0.3, and – 0.97, respectively. (b) active plane interface. The curves 1, 2, 3, and 4 correspond to d =1, 0, – 0.5 and – 0.97, respectively.

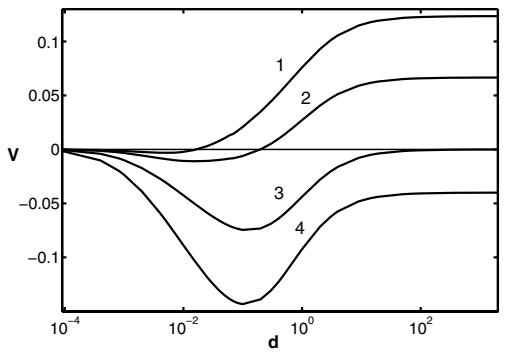

Figure 11 : Velocity of an active drop near an active free surface versus separation distance when $\mu_1 = 1, \mu_2 = 0$ and $\kappa = 1$. The curves 1, 2, 3, and 4 correspond to d =1, 0.5, 0, and – 0.3, respectively.

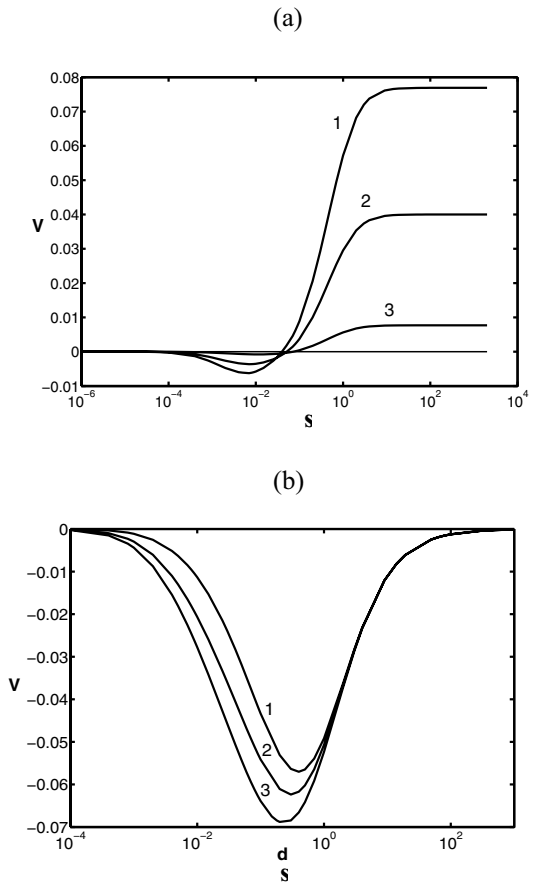

Figure 12 : Migration velocity of a drop in the vicinity of interface versus separation distance when $\mu_2 = 0$, $\kappa = 1$. The curves 1, 2, and 3 correspond to d =0.3, μ_1= 8, 1, and 0.2, respectively. (a) active drop. (b) active outer surface.

Note that due to the linearity of the problem the general case, when the both surfaces are active, may be obtained by superposition of the two special cases mentioned above. Different curves of each plot are calculated for different positions of the source.

One can see that in the case of an active drop's interface, Figure 10a, the dependence of the migration velocity on the separation distance is similar to that in the case of a solid wall. Thus, if the source is located near the upper interface (see curves 1 and 2), the drop migrates from the wall with a velocity growing monotonically with the separation distance up to value of the velocity in the unbounded fluid far from the outer boundary. A source located at the center (line 3), which induces a uniform distribution of concentration at the interface of the drop

and no Marangoni flow in an unbounded fluid, results in the attraction of the drop to an insulated interface. If the source is located lower than the center (lines 4 and 5), the drop moves towards the insulated plane. The migration velocity vanishes at contact and tends to the velocity in unbounded fluid with the growth of separation distance. It is not monotonic, achieving its maximum value at a certain separation of $O(0.1)$. The magnitude of the velocity is larger than in the vicinity of solid wall growing with the decrease of the viscosity of the outer fluid, μ_2 up to the maximum value at the free surface case, $\mu_2 = 0$, as illustrated in Figure 11.

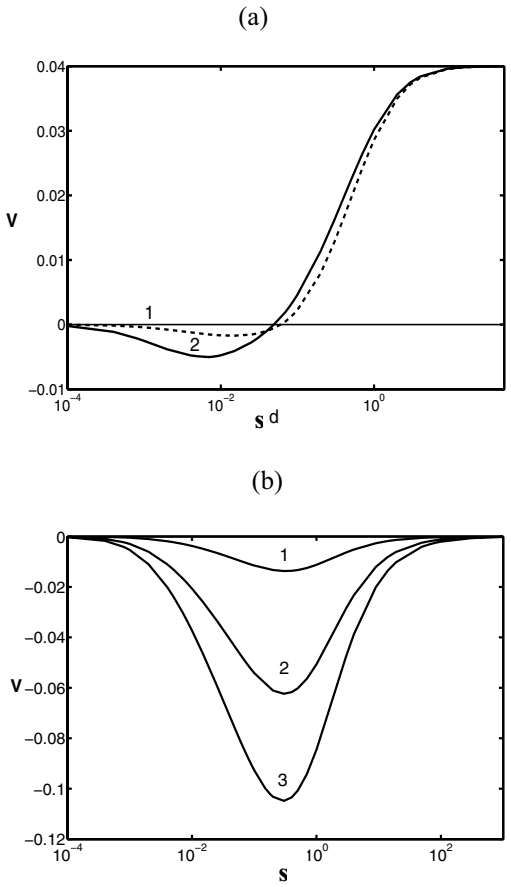

Figure 13 : Migration velocity of a drop in the vicinity of interface versus separation distance when μ_1= 1, κ = 1, and d =0.3 (a) active drop. The curves 1 and 2 correspond to μ_2= 20 and 0.2, respectively. (b) active outer surface. The curves 1, 2, and 3 correspond to μ_2= 8, 1, and 0.2, respectively.

When the interface of the drop is passive, Figure 10b, the flow is induced by the Marangoni flow at the active outer surface. In this case, the direction of drops motion is independent of the position of the source. The drop migrates towards the plane with the migration velocity vanishing at large and small separation distances. At fixed separation, the velocity is larger for lower position of internal source. The magnitude of the velocity exceeds that in the case of active drop. It increases with the decrease of the viscosity of the outer fluid, μ_2, up to a maximum value at the free surface case, $\mu_2 = 0$, as illustrated in Fig. 11. When both surfaces are active, Fig. 11, the attractive effect of the plane may be compensated by an upward motion induced by the active surface of the drop at some equilibrium position, corresponding to zero migration velocity at curves 1 and 2. This equilibrium is an unsteady one as the drop is attracted for lower locations and migrates upwards for higher ones.

The dependence of the migration velocity on the viscosity ratio between the drop and the surrounding medium and between the two liquids separated by the plane interface at given separation is illustrated in Figures 12 and 13, respectively.

Figs (a) correspond to the case of an active drop, and Figs (b) are calculated for an active outer surface. One can see that the dependence on the viscosity of the drop is much stronger in the first case when the dependence on the viscosity of the outer medium is minor. The magnitude of the velocity decreases with the increase of the drop viscosity μ_1, up to the maximum value at the free surface case, $\mu_1 = 0$, as illustrated in Fig. 12. For the case of an active drop, the velocity vanishes as $\mu_1 \to \infty$, while for the case of active it tends to a nonzero value.

The magnitude of the velocity is larger than in the vicinity of solid wall growing with the decrease of the viscosity of the outer fluid, μ_2, up to the maximum value at the free surface case, $\mu_2 = 0$, as illustrated in Fig. 13.

Summarizing the results of the velocity calculations, one can conclude that a mobile boundary with zero mass flux attracts a drop undergoing spontaneous Marangoni migration. This effect is much more pronounced when the interfacial tension on this boundary depends on the concentration of a secreted surfactant.

5 Discussion and conclusions

We have studied the motion of a drop in the vicinity of a solid or a fluid-fluid boundary. The motion is induced by the internal secretion of a surface-active substance. The

latter distributes non-uniformly on the drop surface and the resulting stress variation drives the locomotion of the drop. Cases of plane and spherical boundaries have been considered as well as cases of linear and non-linear dependence of the interfacial tension on the concentration of the surfactant. The dependence of the drop migration velocity on the location of the source and on the separation distance between the drop and the outer boundary, as well as on the physical parameters of the system, is reported. The dynamics of the drop is studied in the case of a fixed location of the source inside the drop, and in the case when it passively moves with the internal circulation.

The interaction between suspended particles and boundaries in viscous flow is a subject with a rich literature. In this section we compare our results to those available in the literature for a particle embedded in various types of motion. We restrict our review to the cases closest to the situation considered in this paper, i.e. creeping flow induced solely by the motion of a droplet settling in a gravity field or undergoing thermocapillary migration.

In the sedimentation problems, an external force exerted on a particle does not depend on its position with respect to the boundary that affects solely a viscous resistance to the motion. A comprehensive introduction to the topic can be found in Happel and Brenner (1965). Bart (1968), who studied the case of a fluid drop settling towards a liquid-liquid interface, demonstrated that the presence of a nearby boundary strongly increases viscous drag on a droplet. For a near contact configuration, the drag force asymptotic behavior was studied, making use of the lubrication approximation analysis, by Davis, Schonberg and Rallison (1989) and by Barnocky and Davis (1989). It was found that, when the separation distance tends to zero, viscous drag on an undeformable particle tends to infinity as s^{-1} for a solid wall and as $s^{-1/2}$ for a mobile interface. Thus it takes a drop a finite time to fall on a mobile interface and infinite time to contact a solid wall. The effects of slight deformability of the drops were studied by Yiantsios and Davis (1991) and by Loewenberg and Davis (1993), while the influence of the wall roughness was the subject in Zhao, Galvin and Davis (2002) and Zhao and Davis (2003).

The main difference between sedimentation and thermocapillary migration is that, in the latter case, not only viscous resistance but also the temperature distribution and hence "thermocapillary force" depends on the geometry of the system. Bi-spherical coordinates were employed to determine thermocapillary migration velocity of a bubble or droplet perpendicular to an isothermal planar solid and free surface in Keh and Chen (1990) and Barton and Subramanian (1990, 1991). Asymptotic solutions of this problem were obtained by Chen and Keh (1990) and Chen (1999a) using the reflection method and by Loewenberg and Davis (1993) employing lubrication approach. These results were extended to the cases of thermocapillary migration parallel to an insulated plane in Chen (1999b) and to the migration in an arbitrary direction with respect to a planar surface with constant temperature gradient by Meyyappan and Subramanian (1987) and by Chen (2000). The effect of the deformability of a drop has been studied in Ascoli and Leal (1990), while thermocapillary motion of a drop between two plane walls was the subject of Keh and Chen (2001, 2002). Summarizing findings of the researches mentioned above, it was demonstrated that, though the boundary effect on the thermocapillary motion is much weaker than on the motion driven by body force, the former becomes significant for small separations. For a droplet moving normal to a plane wall, the velocity is always smaller than that of a particle isolated in an unbounded domain. In contrast to this, the presence of a wall can be an enhancement factor for the translation in the parallel direction. The effect of the presence of a passive free surface can be either retarding or enhancing depending on the parameters of the process.

In this paper it was demonstrated that, similar to the motion under external temperature gradient, the presence of a nearby boundary affects both the hydrodynamic resistance to the drops motion and temperature/surfactant distribution over its interface and, hence, the Marangoni force. The boundaries increase the hydrodynamic resistance to the flow and, thus, fluid flow near the boundary has lower velocity as compared to those in unbounded medium for the same external forcing. On the other hand, for the surface induced flow, a nearby boundary affects the concentration at the drops surface and hence the Marangoni flow. Our calculations revealed that the boundary with constant concentration has a repulsive effect on the drop, while an insulated boundary tends to attract a drop. For a large separation distance, the motion of the drop is similar to that in an unbounded fluid, while for smaller separations it is considerably retarded and, in some cases, can be even reversed. For the latter

cases there exists an equilibrium separation corresponding to zero migration velocity. In the case of a constant concentration, this equilibrium is stable for a fixed source position and it is unstable when the source is freely suspended.

Note that in the case of thermocapillary migration under external temperature gradient as well as in the case of settling under gravity, the presence of nearby boundaries affects only the magnitude of the migration velocity while the direction remains the same as for an isolated drop. In contrast to this, for the self-induced thermocapillarity, even the direction of the drop's motion may be changed by the presence of a boundary.

Free surface and a liquid/liquid interface differ from a solid wall in two main aspects: First, it is mobile, i.e. tangential velocity on the interface does not vanish and, hence, its retardation effect on the flow is less pronounced than that of a solid boundary. Second, its surface tension may depend on concentration as well as it is at the drops interface. In this case, the Marangoni flow is induced not only at the vicinity of the drop, but also at the vicinity of the boundary. This flow is shown to be quite strong being able to change the flow pattern and the direction of the drops migration. Similar effect was described by Golovin (1995) and by Leshansky, Golovin, Nir (1997) who described the flow induced by a hot solid particle near a free surface resulting in a thermocapillary induced migration of the solid particle.

When the interface of the drop is passive, the motion is induced by the Marangoni flow at the active outer surface. In this case, the direction of drops motion is independent of the position of the source. The drop migrates towards the plane with the migration velocity vanishing at large and small separation distances. At fixed separation, the velocity is larger for lower position of the internal source. The magnitude of the velocity exceeds the one in the case of an active drop. It increases with the decrease of the viscosity of the outer fluid, $\mu_{2,}$ up to the maximum value at a free surface case, $\mu_2 = 0$. When both surfaces are active, the attractive effect of the plane may be compensated by an upward motion induced by the active surface of the drop at some equilibrium position, corresponding to zero migration velocity. This equilibrium is an unsteady one as the drop is attracted for lower locations and migrates upwards for higher ones.

Summarizing the results of the velocity calculations, one can conclude that mobile interface with zero mass flux attracts a drop undergoing spontaneous Marangoni migration. This effect is much more pronounced when the interfacial tension on this boundary depends on the concentration of the secreted surfactant.

Most of the results presented are computed for a linear dependence of surface tension on concentration. Sample calculations were also performed for a non-linear case, taking into account the slowing down of the change of surface tension with concentration at near saturation situation. A quasi-linear model was admitted. It was demonstrated that calculations with the linear surface tension provide upper bound for the migration velocity. As anticipated, the non-linear dependence of surface tension results in slowing down of the Marangoni flow, which is completely suppressed when the interface is saturated by surfactants. For the motion induced by the internal secretion, this effect is much more pronounced when the source is located closer to the interface and the larger part of the interface has a high concentration.

In practice, the non-linear dependence of surface tension on a surfactant concentration is not of a quasi-linear nature but a convex curve that lies above some low critical tension (see e.g. Adamson, 1990). Though our calculations were performed for a simplified surface tension dependence, this dependence reflects some characteristic features of the physics of the problem as the convexity of $\sigma(C)$ curve and a positive constant tension above some critical concentration .

Acknowledgement: The research was supported by ISF grant 74/01. DTs and OML acknowledge the support of the Israel Ministry for Immigrant Absorption. The authors thank Mr. A. Gorbovich who performed computation cited in section 4.1.2.

References:

Adamson, A. W. (1990): Physical Chemistry of Surfaces, Fifth edition Wiley, New York.

Ascoli, E. P.; Leal. L. G. (1990): Thermocapillary motion of a deformable drop towards a planar wall. *J. Colloid Interf. Sci.*, vol. 138, pp. 220-230.

Barnocky, G.; Davis, R. H. (1989): The lubrication force between spherical drops, bubbles and rigid particles in viscous flow. *Int. J. Multiphase Flow* vol. 15, pp. 627-638.

Bart, E., (1968): The slow unsteady settling of a fluid

sphere towards a flat fluid interface. *Chem. Eng Sci.*, vol. 23, pp. 193-210.

Barton, K. D.; Subramanian, R. S. (1990): Thermocapillary migration of a liquid drop normal to a plane surface. *J. Colloid Interf. Sci.* vol. 137, pp. 170-182.

Barton, K. D.; Subramanian, R. S. (1991): Migration of liquid drops in a vertical temperature gradient: interaction effects near a horizontal surface. *J. Colloid Interf. Sci.,* vol. 141, pp. 146-156.

Chen, S. H. (1999a): Thermocapillary deposition of a fluid droplet normal to a planar surface. *Langmuir*, vol. 15, pp. 2674-2684.

Chen, S. H. (1999b): Thermocapillary migration of a fluid sphere parallel to an insulated plane. *Langmuir*, vol. 15, pp. 8618-8626.

Chen, S. H. (2000): Movement of a fluid sphere in the vicinity of a flat plane with constant temperature gradient, *J. Colloid Interf. Sci.*, vol. 230, pp.157-170.

Chen, S. H.; Keh, H. J. (1990): Thermocapillary motion of a fluid droplet normal to a plane surface. *J. Colloid Interf. Sci.*, vol. 137, pp. 550-562.

Chen, S. H.; Stebe, K. J. (1997): Surfactant-induced retardation of the thermocapillary migration of a droplet *J. Fluid Mech.*, vol. 304, pp. 35-59.

Davis, R. H.; Schonberg, J. A.; Rallison, J. M. (1989): The lubrication force between two viscous drops. *Ph. Fluids A*, vol. 1, pp. 77-81.

Edwards, D. A.; Brenner, H.; Wasan, D. T. (1991): Interfacial Transport Processes and Rheology, Butterworth-Heinemann, Massachusetts.

Golovin, A. A. (1995): Thermocapillary interaction between solid particle and gas bubble. *Int. J. Multiphase Flow*, vol. 21, pp. 715- 719.

Golovin, A. A.; Nir, A.; Pismen, L. P. (1995): Spontaneous motion of two droplets caused by mass transfer. *Ind. Eng. Chem. Res*., vol. 34, pp. 3278-3288.

Haber, S.; Hetsroni, G.; Solan, A .(1973): Low Reynolds number motion of two drops submerged in an unbounded arbitrary velocity field. *Intl J. Multiphase Flow*, vol. 4, pp. 627-638.

Happel, J.; Brenner, H. (1965): Low Reynolds Number Hydrodynamics. Englewood Cliffs, N. J.:Prentice-Hall.

Keh, H. J.; Chen, S. H. (1990): The axisymmetric thermocapillary motion of two fluid droplets. *Int. J. Multiphase Flow,* vol. 16, pp. 515-527.

Keh, H. J.; Chen, P. Y. (2001): Slow motion of a droplet between two parallel plane walls. *Chem. Engng. Sci*., vol. 56, pp. 6863-6871.

Keh, H. J.; Chen, P. Y.; Chen, L. S. (2002): Thermocapillary motion of a fluid droplet parallel to two plane walls. *Int. J. Multiphase Flow*, vol. 28, pp. 1149-1175.

Leshansky, A., M.; Golovin, A. A.; Nir, A. (1997): Thermocapillary interaction of a solid particle and a liquid-gas interface. *Physics of Fluids*, vol. 9, pp. 2818-2827.

Loewenberg, M.; Davis, R. H. (1993): Near-contact thermocapillary migration of a non-conducting, viscous drop normal to a planar interface. *J. Colloid Interf. Sci*., vol. 160, pp. 265-274.

Meyyappan, M.; Subrananian, R. S. (1987): Thermocapillary migration of a gas bubble in an arbitrary direction with respect to a plane surface. *J. Colloid Interf. Sci.*, vol. 115, pp. 206-219.

Nir, A.; Lavrenteva, O. M. (2003): Capsule dynamics and interfacial transport. In: C. Pozrikidis (ed) *Modeling and Simulation of Capsules and Biological Cells*, CRC Press, pp. 197 –262.

Subrananian, R. S.; Balasubramaniam, R. (2001): *The Motion of Bubbles and Drops in Reduced Gravity.* Cambridge University Press.

Tsemakh, D.; Lavrenteva, O. M.; Nir, A. (2004): On the locomotion of a drop, induced by the internal secretion of surfactant. *Int. J. Multiphase Flow*, vol. 30, pp. 1337-1367.

Yiantsios, S. G.; Davis, R. H. (1991): Close approach and deformation of two viscous drops due to gravity and van der Waals forces. *J. Colloid Interface Sci.*, vol. 144, pp. 412-433.

Zhao, Y.; Galvin, K. P.; Davis, R. H. (2002): Motion of a sphere down a rough plane in a viscous fluid. *Int. J. Multiphase Flow*, vol. 28, pp. 1787-1800.

Zhao, Y.; Davis, R. H. (2003): Interaction of sedimenting particles with multiple surface roughness scales. *J. Fluid Mech.,* vol. 492, pp. 101-129.

Appendix A: Bi-spherical coordinates

Substituting series representation (23) and (25) into the boundary conditions (3) and (4), which correspond to the constant concentration at the outer boundary, results in the following infinite system of linear algebraic equations

$$E_n^1 + G_n^1 = 0, \tag{29}$$

$$(E_n^1 - E_n^0)\cosh(n+\frac{1}{2})\alpha + (G_n^1 - G_n^0)\sinh(n+\frac{1}{2})\alpha = 0, \tag{30}$$

$$G_n^0 \tanh(n+\frac{1}{2})\beta + E_n^0 = 0, \tag{31}$$

$$\begin{aligned}&\sinh(n+\frac{3}{2})\alpha(E_n^0 - E_{n+1}^0) + \cosh(n+\frac{3}{2})\alpha(G_n^0 - G_{n+1}^0)\\ &\quad - \kappa\exp[-(n+\frac{3}{2})\alpha](E_n^1 - E_{n+1}^1)\\ &\quad + \frac{n}{n+1}\left\{\begin{array}{c}\sinh(n-\frac{1}{2})\alpha(E_n^0 - E_{n-1}^0)\\ +\cosh(n-\frac{1}{2})\alpha(G_n^0 - G_{n-1}^0)\\ -\kappa\exp[-(n-\frac{1}{2})\alpha](E_n^1 - E_{n+1}^1)\end{array}\right\}\\ &\quad = \kappa(2n+1)\int_{-1}^{1}(\cosh\alpha - \mu)^{1/2}G(\alpha,\mu)d\mu,\end{aligned} \tag{32}$$

In the case of zero mass flux from the outer boundary (A3) should be replaced by

$$\begin{aligned}&\sinh(n+\frac{3}{2})\beta(E_n^0 - E_{n+1}^0) + \cosh(n+\frac{3}{2})\beta(G_n^0 - G_{n+1}^0)\\ &\quad + \frac{n}{n+1}\left[\begin{array}{c}\sinh(n-\frac{1}{2})\beta(E_n^0 - E_{n-1}^0)\\ +\cosh(n-\frac{1}{2})\beta(G_n^0 - G_{n-1}^0)\end{array}\right] = 0.\end{aligned} \tag{33}$$

To solve this system numerically, we can fix the number of terms, for example N, and assume $E_n = 0$ for $n > N$. By solving the resulting finite system, the coefficients $E_1^0, E_2^0, ..., E_N^0, E_1^1, E_2^1, ..., E_N^1$; $G_1^0, G_2^0, ..., G_N^0$; $G_1^1, G_2^1, ..., G_N^1$ can be found. Increasing the number N, the solution can be found with a desired accuracy.

As soon as the concentration field is available, the stream function can be determined in the form (27), (28). Substituting (27) - (28) into boundary conditions (19) – (21), where the tangential component of the viscous stress tensor, used in (19) and (21) are of the form

$$\Pi_{\xi\zeta} = h\left(\frac{\partial U_\xi}{\partial\zeta} + \frac{\partial U_\zeta}{\partial\xi}\right) + \frac{1}{\sinh\alpha}\left(U_\zeta\sin\xi + U_\xi\sin\zeta\right),$$

results in the following finite system of linear equations for the coefficients of the stream function expansion at any n. The right-hand side of this system depends on the coefficients E_n^i and G_n^i (Golovin, Nir and Pismen, 1995).

$$A_n^1 = -B_n^1, \quad C_n^1 = D_n^1, \quad A_n^2 = B_n^2, \quad C_n^2 = -D_n^1, \tag{34}$$

$$\begin{aligned}W_n^1(\alpha) &= W_n^0(\alpha)\\ &= -\frac{Vn(n+1)\sqrt{2}\sinh\alpha}{2}\left(\frac{e^{-(n-1/2)\alpha}}{2n-1} - \frac{e^{-(n-1/2)\alpha}}{2n+3}\right),\end{aligned} \tag{35}$$

$$W_n^2(\beta) = W_n^0(\beta) = 0, \tag{36}$$

$$\frac{dW_n^i}{d\xi} - \frac{dW_n^0}{d\xi} = 0, \quad \xi = \alpha,\beta, \quad i = 1,2, \tag{37}$$

$$\begin{aligned}&\frac{d^2W_n^0}{d\xi^2} - \mu_1\frac{d^2W_n^1}{d\xi^2} = \frac{n(n+1)(2n+2)}{2}\\ &\quad\times\left[\begin{array}{c}\frac{\sqrt{2}}{2}V(1-\mu_1)\sinh^2\alpha\left(\frac{2\cosh\alpha}{2n+1} - \sinh\alpha\right)\\ \times e^{-(1+1/2)\alpha} + \int_{-1}^{1}\frac{C_{n+1}^{-1/2}(\mu)}{(\cosh\xi-\mu)^{1/2}}\frac{\partial\sigma}{\partial\mu}d\mu\end{array}\right], \xi = \alpha\end{aligned} \tag{38}$$

$$\begin{aligned}&\frac{d^2W_n^0}{d\xi^2} - \mu_2\frac{d^2W_n^2}{d\xi^2}\\ &\quad = \frac{n(n+1)(2n+2)}{2}M\int_{-1}^{1}\frac{C_{n+1}^{-1/2}(\mu)}{(\cosh\xi-\mu)^{1/2}}\frac{\partial\sigma}{\partial\mu}d\mu,\\ &\quad \xi = \beta.\end{aligned} \tag{39}$$

Note that the last equation (39) is presented here in the most general form corresponding to the outer boundary separating two viscous media. The case of a free boundary corresponds to $\mu_2 = 0$,while for a rigid wall 39 should be replaced by

$$\frac{dW_n^0}{d\xi} = 0, \quad \xi = \beta, \tag{40}$$

Substitution (28) for W_n^i into (35) - (40) and taking into account (34) yields a system of twelve linear equations for the twelve unknown coefficients $A_n^i, B_n^i, C_n^i, D_n^i$, i =

0,1,2. An integral term in the right-hand side of (38) and (39) was calculated to yield

$$\int_{-1}^{1} \frac{C_{n+1}^{-1/2}(\mu)}{(\cosh\xi-\mu)^{1/2}} \frac{\partial\sigma}{\partial\mu} d\mu = \frac{2U_n(\xi)}{2n+1} + \frac{1}{2}\sum_{j=1}^{\infty} U_j(\xi) \int_{-1}^{1} \frac{P_j(\mu) C_{n+1}^{-1/2}(\mu)}{\cosh\xi-\mu} d\mu, \tag{41}$$

where

$$U_n(\xi) = E_n^i \cosh(n+1/2)\xi + G_n^i \sinh(n+1/2)\xi.$$